Onset of tetrahedral interstitial formation in GaAsN alloys

J. J. P. Cooper,[1] T. Jen,[1] A. Novak,[1] Z. Xi,[1] L. Qi,[1] F. U. Naab,[2] Y. Q. Wang,[3] R. S. Goldman[1*]

[1]*Department of Materials Science and Engineering, University of Michigan, Ann Arbor, Michigan 48109-2136, USA*

[2]*Michigan Ion Beam Laboratory, University of Michigan, Ann Arbor, Michigan 48109-2136, USA*

[3] *Materials Science and Technology Division, Los Alamos National Laboratory, Los Alamos, New Mexico 87545, USA*

March 9, 2024

ABSTRACT

N incorporation mechanisms in $GaAs_{1-x}N_x$ alloys are probed using combined experimental and computational Rutherford Backscattering Spectrometry (RBS) and Nuclear Reaction Analysis (NRA) angular yield scans. For $x_N < 0.025$, in addition to substitutional nitrogen, N_{As}, $(N\text{-}N)_{As}$ and $(N\text{-}As)_{As}$ split interstitials are observed. However, for $x_N \geq 0.025$, evidence for N tetrahedral interstitials, N_{tetra}, emerges. We propose a mechanism for stabilization of N_{tetra} in which the elastic interaction between N_{tetra} and N_{As} is induced by the opposite signs of their misfit volumes. This work opens opportunities for exploring the formation of N_{tetra} and its influence on the properties of a variety of highly mismatched alloys.

*Corresponding Author: rsgold@umich.edu

Dilute nitride semiconductor alloys have drawn significant attention due to the dramatic bandgap reductions induced by dilute N compositions (x_N up to 0.035) while maintaining near lattice-matching with GaAs,[1–6] resulting in their suitability for long-wavelength lasers,[7,8] detectors,[9,10] and ultra-high-efficiency solar cells.[11,12] However, non-substitutional N incorporation has been linked to diminished absorption and emission efficiencies, in dilute nitride films, GaAsN-based heterostructures, and GaAsPN and GaAsNBi solar cell devices, with partial recovery induced by post-growth annealing.[11–15] Meanwhile, most computational studies have focused on the relative stabilities of substitutional nitrogen (N_{As}) and $(N\text{-}N)_{As}$ and $(N\text{-}As)_{As}$ split interstitials,[16–20] with minimal consideration of N tetrahedral interstitials (N_{tetra}).[16,17] To date, nuclear reaction analysis (NRA) and x-ray photoelectron spectroscopy (XPS) have revealed ~20% non-substitutional N incorporation, as both $(N\text{-}As)_{As}$ and $(N\text{-}N)_{As}$ split interstitials, independent of film growth method,[15,21–24] with the non-substitutional N fraction reduced by post-growth annealing.[15,25,26] Channeling NRA (NRA/c) supported by Monte Carlo-Molecular Dynamics (MCMD) simulations suggests a dominant N interstitial complex aligned along the [010] direction in GaAsN and GaAsNBi alloys.[21,23] Although the [010]-oriented N interstitial complex is typically attributed to $(N\text{-}As)_{As}$, electronic structure calculations suggest that $(N\text{-}N)_{As}$ may also be oriented along the [010] direction.[16,18–20] Furthermore, due to the inability of XPS to distinguish N_{As} from N_{tetra}, and the limited consideration of N_{tetra} in earlier studies, direct detection of N_{tetra} has not been reported.

In this work, we use combined experimental and computational NRA and Rutherford backscattering spectrometry (RBS/c) angular yield scans to investigate the N composition (x_N) dependence of N incorporation mechanisms in GaAsN. For the lowest x_N, in addition to N_{As}, both $(N\text{-}N)_{As}$ and $(N\text{-}As)_{As}$ split interstitials are apparent. However, for $x_N \geq 0.025$, evidence for N_{tetra}

emerges. We discuss the role of N solute atom-induced strain fields as the driving force for N_{tetra} formation. This work opens opportunities for consideration of N_{tetra} and its influence on the properties of a variety of highly mismatched alloys.

A series of 300 nm $GaAs_{1-x}N_x$ films were grown by molecular-beam epitaxy on semi-insulating (001) GaAs substrates, using solid Ga and As_2, and an N_2 rf plasma source, as described elsewhere.[22] Simultaneous NRA and RBS measurements were conducted using 4.5 or 4.64 MeV α particles generated in NEC or General Ionics tandem accelerators, both equipped with fully-automated 5-axis goniometers. For RBS, backscattered α particles were detected by a silicon (Si) surface-barrier detector located at 170° (for 4.5 MeV α) or 167° (for 4.64 MeV α), with respect to the incident beam. For NRA, the yields of the $^{14}N(\alpha,p)^{17}O$ reaction emitted protons were detected by a Si surface-barrier detector located at 135° with respect to the incident beam, with scattered α particles filtered out by 18 μm aluminum or 25.4 μm Kapton. RBS and NRA yields vs. particle energy were measured in the [100], [110], and [111] directions, with random (non-channeling) conditions achieved by oscillating the specimen ±4° away from the channeling condition in θ and φ.[23] In addition, the angular-dependence of RBS and NRA yields (so-called "angular yield scans") were measured at ±1.5° about the [100], [111], and [110] directions.

For each film, N compositions were determined from an analysis of the NRA proton yield versus energy using the simulation of nuclear reaction analysis (SIMNRA) software.[27] The energy-dependent stopping power of α particles[28] was used for energy-to-depth conversion, enabling quantification of the minimum yields, χ_{min} (ratio of aligned yield to random yield), and the angular yield scans, Y(φ), both summed over the depths corresponding to the GaAsN layers (0 to 300 nm). In addition, $Y_{GaAs}(\varphi)$ and $Y_N(\varphi)$ were computed using Monte Carlo-Molecular

Dynamics (MC-MD) simulations with 3 x 3 x 3 supercells of GaAs and $GaAs_{1-x}N_x$ containing 4 N_{As}, 4 N_{tetra}, or 4 $(N\text{-}As)_{As}$, equivalent $x_N = 0.037$.[21,23,29–31]

Analyses of defect-induced stress and calculations of defect binding energies in GaAs were performed by atomistic simulations using the PreFerred Potential (PFP), a high-accuracy universal neural network interatomic potential[32,33] implemented in the Matlantis[34] software package. To compute the stress induced by single point defects, we constructed 3×3×3 cubic supercells of GaAs, containing single N_{As} or N_{tetra}, without relaxations of supercell volumes. In addition, PFP was used to compute the binding energy between isolated N_{As} and N_{tetra} using fully relaxed 6×6×6 cubic supercells.

In Fig. 1, for the (a) [100], (b) [110], and (c) [111] channels, $\chi_{min,\,GaAs}$ and $\chi_{min,\,N}$ are plotted as a function of x_N, with the computed positions of stability for N_{As}, N_{tetra}, $(N\text{-}As)_{As}$, and $(N\text{-}N)_{As}$ shown beneath each plot.[16] For all three channeling directions, N_{As} is shadowed by the GaAs lattice, and $(N\text{-}As)_{As}$ and $(N\text{-}N)_{As}$ are displaced into the channels. Similarly, in the (a) [100] and (c) [111] directions, N_{tetra} is shadowed by the GaAs lattice, observable only in the (b) [110] channel. As shown in the plots, in all cases, $\chi_{min,\,GaAs} = 0.05 \pm 0.02$, suggesting minimal displacement of Ga and As atoms into the [100], [110], and [111] channels, independent of x_N. For the (a) [100] and (c) [111] directions, $\chi_{min,\,N}$ values decrease monotonically with x_N, suggesting a N-dependent decrease in $[(N\text{-}As)_{As}]$ and $[(N\text{-}N)_{As}]$. However, for the (b) [110] direction, $\chi_{min,\,N}$ initially decreases with x_N but finally increases for $x_N \geq 0.025$. Since N is displaced into the [110] channel but not into the [100] and [111] channels, the presence of N_{tetra} must be considered, similar to the cases of Er_{tetra} in GaAs and N_{tetra} in ZnSe.[35,36]

To further explore atomic displacements into the channels, we consider the $Y_{GaAs}(\varphi)$ (open circles) and $Y_N(\varphi)$ (closed squares) about the (a) [100], (b) [110], and (c) [111] channels, shown

in Fig. 2. For GaAs, a minimum in $Y_{GaAs}(\varphi)$, $Y_{min,\ GaAs}$, illustrated as a dashed horizontal line in Fig. 2 (a), is apparent at 0°, where the incident beam is aligned with the channel. The half-width at half-depth, $\Psi_{1/2}$, is illustrated with a horizontal arrow in Fig. 2 (b). For GaAs, $\Psi_{1/2\ [110]} > \Psi_{1/2\ [100]} \sim \Psi_{1/2\ [111]}$, consistent with predictions of $\Psi_{1/2} \propto 1/d_{hkl}^{1/2}$.[37]

For the [100] and [111] channels, $Y_{min,\ GaAs}$ and $\Psi_{1/2,\ GaAs}$ are essentially independent of x_N for the GaAsN layers (Figs. 2 (a) and (c)), consistent with the $\chi_{min,\ GaAs}$ data presented in Fig. 1. Meanwhile, for the [100] and [111] channels, the values of $Y_{min,\ N}$ decrease with x_N then plateau for $x_N \geq 0.021$, presumably due to decreased $[(N\text{-}As)_{As}]$ and $[(N\text{-}N)_{As}]$. For the (a) [100], (b) [110], and (c) [111] channels, $Y_{min,\ N} > Y_{min,\ GaAs}$, consistent with the presence of $(N\text{-}As)_{As}$ and $(N\text{-}N)_{As}$ in all layers.

For the [110] channel, shown in Fig. 2 (b), for low x_N, $Y_{min,\ GaAs}$ and $\Psi_{1/2,\ GaAs}$ are independent of x_N, but dramatically increase for $x_N \geq 0.025$, indicating displacement of Ga and/or As into the [110] channel. Similarly, for GaAsN, the $Y_{min,\ N}$ increases for $x_N \geq 0.025$, indicating an increase in N displaced into the [110] channel. In addition, for $x_N = 0.032$, "flux-peaking" features, i.e. increases in $Y_{min,\ GaAs}$ and $Y_{min,\ N}$, are labelled with downward pointing arrows at -0.3 and +0.3°. The presence of flux-peaking features in the [110] $Y(\varphi)$ is consistent with the presence of tetrahedral interstitials in the zinc blende lattice.[38]

To support the hypothesis for N_{tetra} formation in GaAsN alloys with $x_N \geq 0.025$, we compare MC-MD simulations of $Y_{GaAs}(\varphi)$ and $Y_N(\varphi)$ (Fig. 3) for (a) [100], (b) [110], and (c) [111] channels in GaAs (purple) and GaAsN (blue and green), using the predicted positions of N_{As}, N_{tetra}, and $(N\text{-}As)_{As}$.[16] For the computed $Y_{GaAs}(\varphi)$, $\Psi_{1/2\ [110]} > \Psi_{1/2\ [100]} \sim \Psi_{1/2\ [111]}$, consistent with the measured values (above) and predictions of $\Psi_{1/2} \propto 1/d_{hkl}^{1/2}$.[37]

For GaAsN, weighted averages of $Y_{N\_As}(\varphi)$, $Y_{Ntetra}(\varphi)$, and $Y_{(N\text{-}As)\_As}(\varphi)$ were generated assuming 80% substitutional N incorporation. In the case of N incorporation as N_{As} + $(N\text{-}As)_{As}$, shown in blue, the computed values of $Y_{min,\,N}$ ($\Psi_{1/2,\,N}$) are higher (lower) than those of $Y_{min,\,GaAs}$ ($\Psi_{1/2,\,GaAs}$), for all channels, due to the presence of $(N\text{-}As)_{As}$ in the channels. However, for GaAsN containing N_{As} + $(N\text{-}As)_{As}$ + N_{tetra}, shown in green, $Y_{min,\,N}$ ($\Psi_{1/2,\,N}$) are higher (lower) than those of $Y_{min,\,GaAs}$ ($\Psi_{1/2,\,GaAs}$), for the [110] channels, with minimal differences for the [100] and [111] channels, a trend similar to that of the measured $Y_N(\varphi)$.

To estimate the average inter-N separation for N atoms distributed randomly in the GaAs lattice, we use the radius of a sphere occupied by one N atom, termed the Wigner-Seitz radius, r_s,[39,40]

$$r_s = \left[\frac{3}{2\pi \cdot x_N \cdot n_{GaAs}}\right]^{1/3} = 0.391 \cdot x_N^{-1/3} \cdot a_{GaAs} \qquad (1)$$

with GaAs atomic density (n_{GaAs} = 4.44 x 10^{22} atoms/cm^3) and lattice parameter (a_{GaAs} = 0.5633 nm). At the threshold composition for observation of N_{tetra}, x_N = 0.025, with 80% N_{As} incorporation, the computed value of r_s decreases to 0.81 nm. This value is similar to the distance between N_{As} on fourth nearest-neighbor As sites (0.80 nm), whose vibrational modes have been quantified using infrared spectroscopy, suggesting the presence of long-range elastic interactions between N_{As} at this separation.[41]

We now consider the elastic interactions between N solute atoms arising from their misfit volumes. The misfit volume of a solute atom in a crystal is the difference between the volume of the solute atom and its volume on a substitutional or interstitial site. To quantify the effect of misfit volume on N_{tetra} incorporation, we computed the stresses generated by N_{As} and N_{tetra}. Due to its negative (positive) misfit volume, N_{As} (N_{tetra}) generates tensile (compressive) hydrostatic stress of 352 MPa (126 MPa). Thus, the coexistence of N_{As} and N_{tetra} is predicted to minimize the misfit

volume and the corresponding internal stress in GaAsN alloys. Similar arguments have been proposed for strain-induced stabilization of Ga_{tetra} in GaAsN alloys.[42] The stabilization of N_{tetra} in GaAsN is further supported by our computation of N_{As} - N_{tetra} nearest-neighbor binding energy as -0.586 eV.

In summary, we have probed N incorporation mechanisms in $GaAs_{1-x}N_x$ alloys using measured and MC-MD computed $Y_{GaAs}(\varphi)$ and $Y_N(\varphi)$. For all $GaAs_{1-x}N_x$ alloys, N_{As}, $(N\text{-}N)_{As}$ and $(N\text{-}As)_{As}$ are observed, consistent with earlier studies.[15,21,23,24] However, for $x_N \geq 0.025$, evidence for N_{tetra} emerges. With support from atomistic simulations, we propose a stabilization mechanism for N_{tetra} in which its elastic interaction with N_{As} is induced by the opposite signs of their misfit volumes. This work opens opportunities for exploring the stability of N_{tetra} and its influence on the properties and device applications of a variety of highly mismatched alloys.

SUPPLEMENTAL MATERIALS

See the supplemental materials for a description of the energy-to-depth conversion for the RBS yield vs. energy spectra. Values of $Y_{min, GaAs}$ and $Y_{min, N}$, from $Y_{GaAs}(\varphi)$ and $Y_N(\varphi)$ collected about the [100], [110], and [111] channeling directions, are tabulated. We also provide the RBS and NRA yield vs. energy spectra for $GaAs_{1-x}N_x$ layers in the [100], [110], and [111] channeling directions.

ACKNOWLEDGEMENTS

We gratefully acknowledge support from the National Science Foundation (Grant No. DMR 1810280). This work was performed, in part, at the Center for Integrated Nanotechnologies, an Office of Science User Facility operated for the U.S. Department of Energy (DOE) Office of Science. Los Alamos National Laboratory, an affirmative action equal opportunity employer, is managed by Triad National Security, LLC for the U.S. Department of Energy's NNSA, under contract 89233218CNA000001. Z. Xi and L. Qi also gratefully acknowledge support from the Department of Energy (Grant No. DE-SC0023222)

DATA AVAILABILITY

The data that support the findings of this study are mainly available within the article and supplementary materials and from the corresponding author upon reasonable request.

FIGURE CAPTIONS

FIG. 1: $\chi_{min,\ GaAs}$ and $\chi_{min,\ N}$ values for $GaAs_{1-x}N_x$ layers plotted as a function of x_N for the [100] (a), [110] (b), and [111] (c) channels, from Yield vs. Energy spectra measured with 4.64 MeV α. The models shown on the bottom are projections in the [100], [110], and [111] channeling directions for GaAsN unit cells, that contain N_{As}, N_{tetra}, $(N\text{-}As)_{as}$, and $(N\text{-}N)_{As}$, using relaxed positions predicted by density functional theory.[16] The white, green, and blue spheres represent Ga, As, and N respectively.

FIG. 2: Measured Nuclear Reaction Analysis (NRA) angular yields ($Y_N(\varphi)$) (filled squares) and Rutherford Backscattering Spectrometry (RBS) angular yields ($Y_{GaAs}(\varphi)$) (open circles) about the [100] (a), [110] (b), and [111] (c) channels for $GaAs_{1-x}N_x$ with $x_N = 0.006$ to $x_N = 0.032$, measured with 4.5 MeV α.

FIG. 3: Monte Carlo Molecular Dynamics simulations of Nuclear Reaction Analysis (NRA) angular yields ($Y_N(\varphi)$) and RBS angular yields ($Y_{GaAs}(\varphi)$) (top) about the [100] (a), [110] (b), and [111] (c) directions for $GaAs_{1-x}N_x$ containing $x_{N\_As} = 0.03$, $x_{N\_tetra} = 0.0037$, and $x_{(N\text{-}As)\_As} = 0.0037$ (blue) and $x_{N\_As} = 0.03$ and $x_{(N\text{-}As)\_As} = 0.0074$ (green) and for GaAs (purple). Ball-stick models of GaAs unit cell projections (bottom) showing the displacement of N atoms into each channel for N_{tetra}, $(N\text{-}N)_{As}$, and $(N\text{-}As)_{As}$.

References

[1] W.G. Bi, and C.W. Tu, "Bowing parameter of the band-gap energy of GaNxAs1−x," Appl. Phys. Lett. **70**, 1608 (1997).

[2] W. Shan, W. Walukiewicz, J.W. Ager, E.E. Haller, J.F. Geisz, D.J. Friedman, J.M. Olson, and S.R. Kurtz, "Band Anticrossing in GaInNAs Alloys," Phys. Rev. Lett. **82**, 1221 (1999).

[3] E.P. O'Reilly, A. Lindsay, P.J. Klar, A. Polimeni, and M. Capizzi, "Trends in the electronic structure of dilute nitride alloys," Semicond. Sci. Technol. **24**, 033001 (2009).

[4] W. Żuraw, W.M. Linhart, J. Occena, T. Jen, J.W. Mitchell, R.S. Goldman, and R. Kudrawiec, "Temperature-dependent study of GaAs1−x−yNxBiy alloys for band-gap engineering: photoreflectance and k · p modeling," Appl. Phys. Express **13**, 091005 (2020).

[5] T. Taliercio, R. Intartaglia, B. Gil, P. Lefebvre, T. Bretagnon, U. Tisch, E. Finkman, J. Salzman, M.-A. Pinault, M. Laügt, and E. Tournié, "From GaAs:N to oversaturated GaAsN: Analysis of the band-gap reduction," Phys. Rev. B **69**, 073303 (2004).

[6] J. Occena, T. Jen, J.W. Mitchell, W.M. Linhart, E.-M. Pavelescu, R. Kudrawiec, Y.Q. Wang, and R.S. Goldman, "Mapping the composition-dependence of the energy bandgap of GaAsNBi alloys," Appl. Phys. Lett. **115**, 082106 (2019).

[7] M. Gębski, D. Dontsova, N. Haghighi, K. Nunna, R. Yanka, A. Johnson, R. Pelzel, and J.A. Lott, "Baseline 1300 nm dilute nitride VCSELs," OSA Contin. **3**, 1952 (2020).

[8] H. Riechert, A. Ramakrishnan, and G. Steinle, "Development of InGaAsN-based 1.3 μm VCSELs," Semicond. Sci. Technol. **17**, 892 (2002).

[9] A. Albo, D. Fekete, and G. Bahir, "The opportunity of using InGaAsN/AlGaAs quantum wells for extended short-wavelength infrared photodetection," Infrared Phys. Technol. **96**, 68 (2019).

[10] B. Ściana, I. Zborowska-Lindert, D. Pucicki, B. Boratyński, D. Radziewicz, M. Tłaczała, J. Serafińczuk, P. Poloczek, G. Sęk, and J. Misiewicz, "Technology and characterisation of GaAsN/GaAs heterostructures for photodetector applications," Opto-Electron. Rev. **16**, 1 (2008).

[11] K. Yamane, Y. Maki, S. One, A. Wakahara, E.-M. Pavelescu, T. Ohshima, T. Nakamura, and M. Imaizumi, "Mechanism of improved crystallinity by defect-modification in proton-irradiated GaAsPN photovoltaics: Experimental and first-principle calculations approach," J. Appl. Phys. **132**, 065701 (2022).

[12] H. Kawata, S. Hasegawa, J. Matsumura, H. Nishinaka, and M. Yoshimoto, "Fabrication of a GaAs/GaNAsBi solar cell and its performance improvement by thermal annealing," Semicond. Sci. Technol. **36**, 095020 (2021).

[13] S. Fahy, A. Lindsay, H. Ouerdane, and E.P. O'Reilly, "Alloy scattering of n-type carriers in GaNxAs1-x," Phys. Rev. B **74**, 035203 (2006).

[14] E.-M. Pavelescu, O. Ligor, J. Occena, C. Ticoş, A. Matei, R.L. Gavrilă, K. Yamane, A. Wakahara, and R.S. Goldman, "Influence of electron irradiation and rapid thermal annealing on photoluminescence from GaAsNBi alloys," Appl. Phys. Lett. **117**, 142106 (2020).

[15] F. Ishikawa, K. Higashi, S. Fuyuno, M. Morifuji, M. Kondow, and A. Trampert, "Annealing induced atomic rearrangements on (Ga,In) (N,As) probed by hard X-ray photoelectron spectroscopy and X-ray absorption fine structure," Sci. Rep. **8**, 5962 (2018).

[16] K. Laaksonen, H.-P. Komsa, T.T. Rantala, and R.M. Nieminen, "Nitrogen interstitial defects in GaAs," J. Phys. Condens. Matter **20**, 235231 (2008).

[17] E. Arola, J. Ojanen, H.-P. Komsa, and T.T. Rantala, "Atomic and electronic structures of N interstitials in GaAs," Phys. Rev. B **72**, 045222 (2005).

[18] J.D. Querales-Flores, C.I. Ventura, and J.D. Fuhr, "Effect of N interstitial complexes on the electronic properties of GaAs 1 − x N x alloys from first principles," Phys. Rev. Mater. **3**, 024602 (2019).

[19] J. Li, X. Han, C. Dong, and C. Fan, "Formation energies of substitutional NAs and split interstitial complexes in dilute GaAsN alloys with different growth orientations," Appl. Phys. A **124**, 108 (2018).

[20] N. Shtinkov, P. Desjardins, R.A. Masut, and M. Côté, "Nitrogen incorporation and lattice constant of strained dilute $GaAs_{1-x}N_x$ layers on GaAs (001): An ab initio study," Phys. Rev. B **74**, 035211 (2006).

[21] T. Jen, G. Vardar, Y.Q. Wang, and R.S. Goldman, "Identifying the dominant interstitial complex in dilute GaAsN alloys," Appl. Phys. Lett. **107**, 221904 (2015).

[22] M. Reason, H.A. McKay, W. Ye, S. Hanson, R.S. Goldman, and V. Rotberg, "Mechanisms of nitrogen incorporation in GaAsN alloys," Appl. Phys. Lett. **85**, 1692 (2004).

[23] J. Occena, T. Jen, E.E. Rizzi, T.M. Johnson, J. Horwath, Y.Q. Wang, and R.S. Goldman, "Bi-enhanced N incorporation in GaAsNBi alloys," Appl. Phys. Lett. **110**, 242102 (2017).

[24] M.C. López-Escalante, B. Ściana, W. Dawidowski, K. Bielak, and M. Gabás, "Atomic configurations in AP-MOVPE grown lattice-mismatched InGaAsN films unravelled by X-ray photoelectron spectroscopy combined with bulk and surface characterization techniques," Appl. Surf. Sci. **433**, 1 (2018).

[25] R.L. Field, Y. Jin, H. Cheng, T. Dannecker, R.M. Jock, Y.Q. Wang, C. Kurdak, and R.S. Goldman, "Influence of N incorporation on persistent photoconductivity in GaAsN alloys," Phys. Rev. B **87**, 155303 (2013).

[26] T. Ahlgren, E. Vainonen-Ahlgren, J. Likonen, W. Li, and M. Pessa, "Concentration of interstitial and substitutional nitrogen in GaNxAs1−x," Appl. Phys. Lett. **80**, 2314 (2002).

[27] M. Mayer, *SIMNRA User's Guide* (Max-Planck-Institut für Plasmaphysik, Garching, 1997).

[28] J.F. Ziegler, and J.P. Biersack, in *Treatise Heavy-Ion Sci. Vol. 6 Astrophys. Chem. Condens. Matter*, edited by D.A. Bromley (Springer US, Boston, MA, 1985), pp. 93–129.

[29] D. Wijesundera, Ion-Beam Channeling in Non-Centrosymmetric Crystals, Ph.D., University of Houston, 2010.

[30] D.N. Wijesundera, Q. Chen, K.B. Ma, X. Wang, B. Tilakaratne, and W.-K. Chu, "Planar channeling in wurtzite structured ZnO (0001): Anisotropic effects due to the non-centrosymmetric structure," Nucl. Instrum. Methods Phys. Res. Sect. B Beam Interact. Mater. At. **281**, 77 (2012).

[31] T. Jen, Ion Beam Analysis of Solute Incorporation in GaAsN and GaAsNBi Alloys, Ph.D., University of Michigan, 2017.

[32] S. Takamoto, C. Shinagawa, D. Motoki, K. Nakago, W. Li, I. Kurata, T. Watanabe, Y. Yayama, H. Iriguchi, Y. Asano, T. Onodera, T. Ishii, T. Kudo, H. Ono, R. Sawada, R. Ishitani, M. Ong, T. Yamaguchi, T. Kataoka, A. Hayashi, N. Charoenphakdee, and T. Ibuka, "Towards universal neural network potential for material discovery applicable to arbitrary combination of 45 elements," Nat. Commun. **13**, 2991 (2022).

[33] S. Takamoto, D. Okanohara, Q.-J. Li, and J. Li, "Towards universal neural network interatomic potential," J. Materiomics **9**, 447 (2023).

[34] Matlantis (https://matlantis.com/), "software as a service style material discovery tool," (2023).

[35] J. Nakata, M. Taniguchi, and K. Takahei, "Direct evidence of Er atoms occupying an interstitial site in metalorganic chemical vapor deposition-grown GaAs:Er," Appl. Phys. Lett. **61**, 2665 (1992).

[36] H. Kobayashi, K. Kimura, F. Nishiyama, S. Miwa, and T. Yao, "Lattice location of N in ZnSe by channeling-NRA," Nucl. Instrum. Methods Phys. Res. Sect. B Beam Interact. Mater. At. **132**, 142 (1997).

[37] W.-K. Chu, J.W. Mayer, and M.-A. Nicolet, in *Backscattering Spectrom.*, edited by W.-K. Chu, J.W. Mayer, and M.-A. Nicolet (Academic Press, 1978), pp. 223–275.

[38] H. Krause, M. Lux, E. Nowak, J. Vogt, R. Flagmeyer, G. Kühn, and G. Otto, "Lattice Site Localization of Zn in InP Using the PIXE/Channeling Technique," Phys. Status Solidi A **132**, 295 (1992).

[39] J.M. Ziman, in *Models Disord. Theor. Phys. Homog. Disord. Syst.* (Cambridge University Press, Cambridge [Eng.] ; New York, 1979), pp. 472–474.

[40] P.-G. Reinhard, and E. Suraud, in *Introd. Clust. Dyn.* (John Wiley & Sons, Ltd, 2003), pp. 259–266.

[41] A. Carvalho, S.J. Barker, R. Jones, R.S. Williams, M.J. Ashwin, R.C. Newman, P.N. Stavrinou, G. Parry, T.S. Jones, S. Öberg, and P.R. Briddon, "Identification of the local vibrational modes of small nitrogen clusters in dilute GaAsN," Phys. B **401**, 339 (2007).

[42] P. Laukkanen, M.P.J. Punkkinen, J. Puustinen, H. Levämäki, M. Tuominen, K. Schulte, J. Dahl, J. Lång, H.L. Zhang, M. Kuzmin, K. Palotas, B. Johansson, L. Vitos, M. Guina, and K. Kokko, "Formation and destabilization of Ga interstitials in GaAsN: Experiment and theory," Phys. Rev. B **86**, 195205 (2012).

PLEASE CITE THIS ARTICLE AS DOI: 10.1063/5.0192454

FIG 1

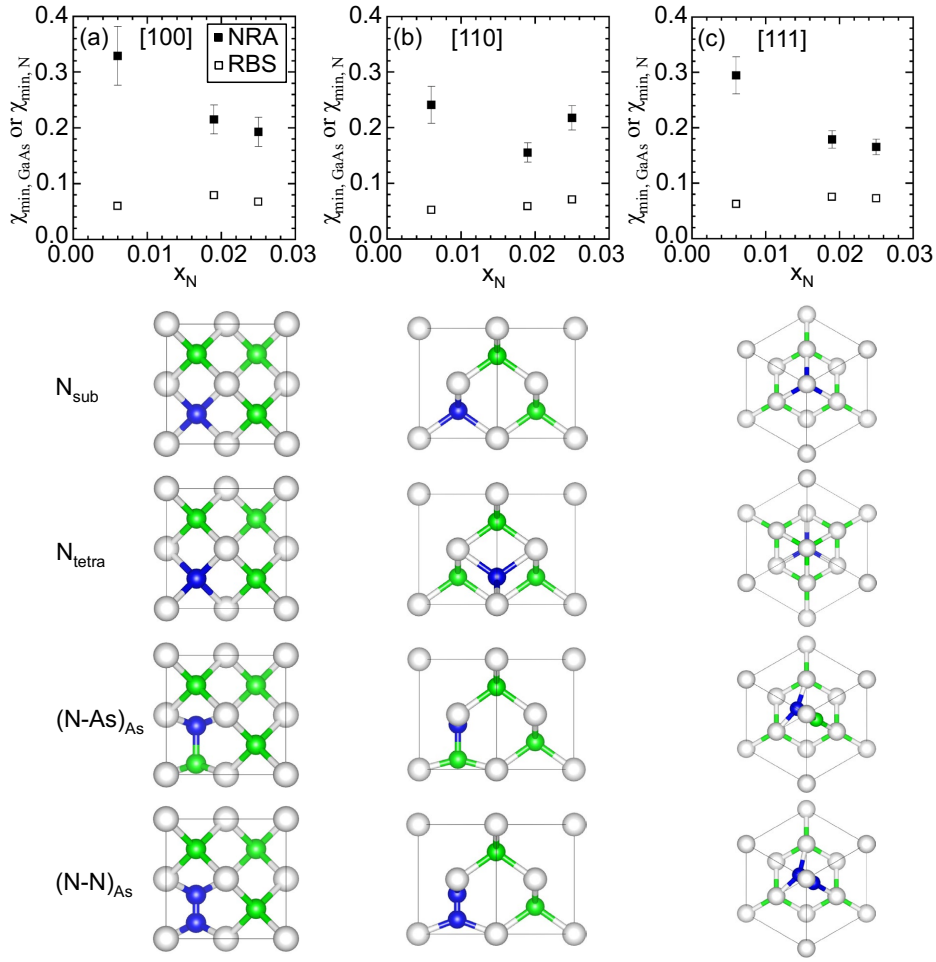

FIG 2

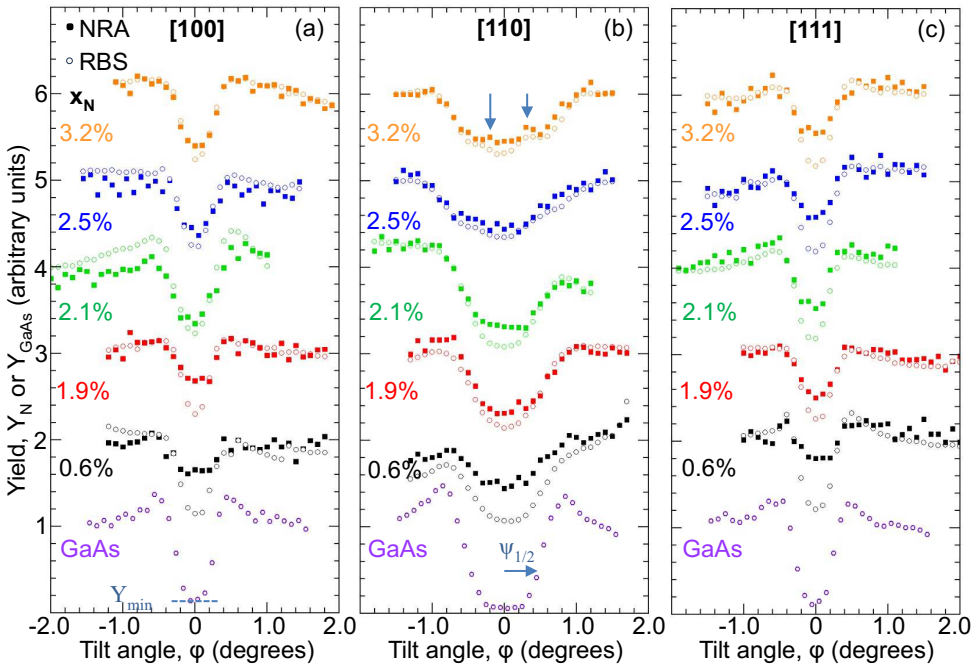

FIG 3